

Efficient metal-free sensitizers bearing circle chain embracing π -spacers for dye-sensitized solar cells†

Cite this: DOI: 10.1039/c3ta12368e

Jian Liu,^a Xudong Yang,^a Ashraf Islam,^a Youhei Numata,^a Shufang Zhang,^a Noviana Tjitra Salim,^a Han Chen^b and Liyuan Han^{*ab}

The circle chain embracing D- π -A dyes have been demonstrated as a promising type of sensitizer for dye-sensitized solar cells (DSCs). To further develop this type of organic dye for DSCs and discover the heuristic points on energy level matching, we introduced various donor moieties (carbazole, indoline and dimethoxytriphenylamine) into a D- π -A system bearing a circle chain embracing a π -spacer and cyanoacrylic acid as an acceptor, resulting in three new organic dyes **LJ-4**, **LJ-5** and **LJ-6**, respectively. Among these dyes, the energy levels of the molecular orbitals in carbazole dye **LJ-4** match best with the conduction band of TiO₂ and the redox potential of the redox species. DSCs employing the sensitizer **LJ-4** and the iodine redox electrolyte exhibit a high power conversion efficiency of 9.20%, measured under the 100 mW cm⁻², simulated AM1.5 sunlight. This work highlights the importance of energy level matching in the further molecular design of a circle chain embracing D- π -A dyes.

Received 18th June 2013

Accepted 3rd July 2013

DOI: 10.1039/c3ta12368e

www.rsc.org/MaterialsA

Introduction

Dye-sensitized solar cells (DSCs), a type of innovative photo-voltaic device with an operating principle resembling the natural photosynthetic process, are considered to be the next generation of photovoltaics due to their potential applications in cost-efficient renewable energy, as well as in the production of electronics. Since the pioneering report in 1991,¹ unremitting research effort has been devoted to this type of device, resulting in significant progress, in molecular engineering,² investigation of the mechanism,³ and the recorded efficiencies continue to increase.⁴ In order to avoid the use of noble metals and having to face the environmental issues that follow, metal-free organic D- π -A dyes have emerged, and DSCs based on organic dyes have yielded competitive conversion efficiencies up to 9%.⁵ Achieving higher efficiencies, which involves the improvement of open-circuit voltage and short-circuit current, is required for practical application. However, such improvements have been considered as the most important and challenging subject in the development of organic sensitizers.⁶

In order to overcome the common issues involving aggravated intermolecular interactions and charge recombination, which deteriorate photocurrent generation and decrease

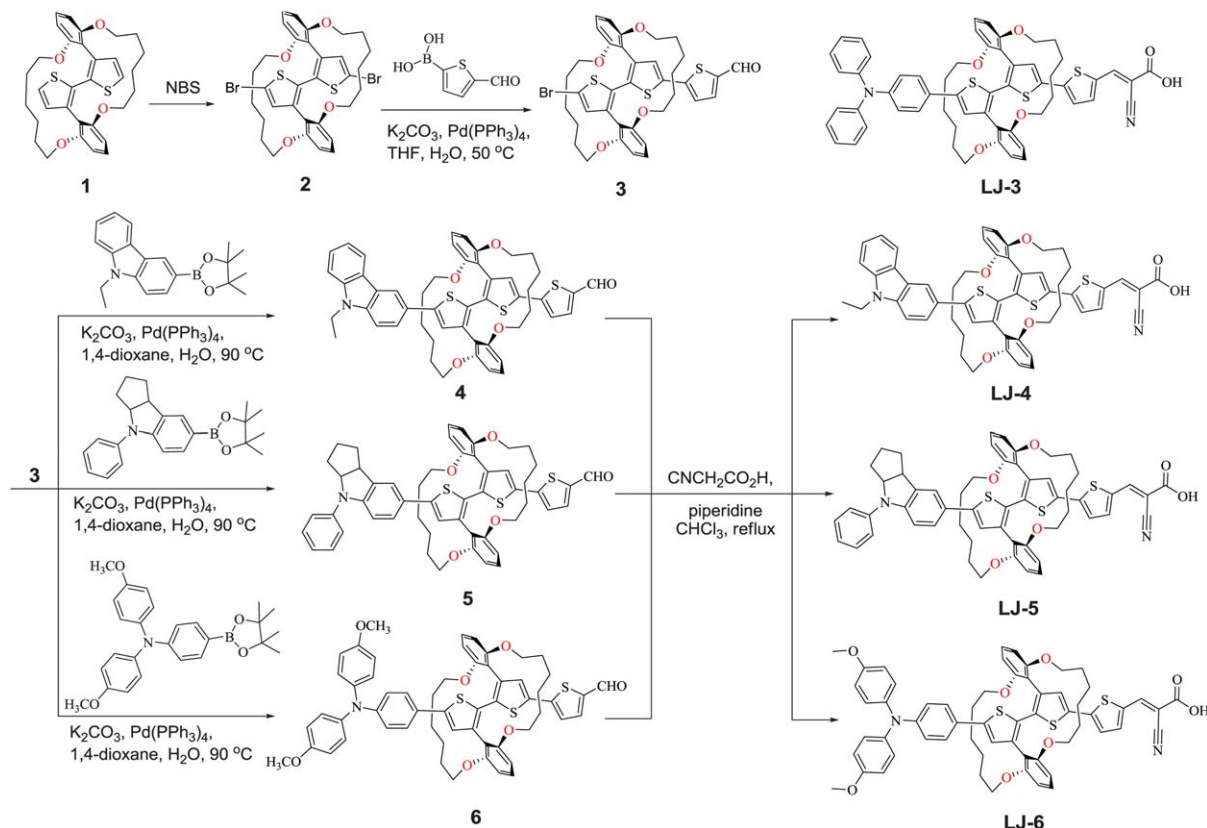
photovoltage in DSCs based on organic D- π -A dyes,⁷ the introduction of steric hindrance on the dye molecule has been demonstrated as an effective strategy in molecular design.^{2c,8} Currently, two styles of substituent are adopted for steric hindrance in organic D- π -A dyes. One is the flexible bulky groups (alkyl chains, *etc.*) side linked on the donor part and/or π -conjugated backbone,^{2c,8a,c} and another is the rigid circle chain surrounding the π -spacer.⁹ The former has been discussed to be effective in suppressing the intermolecular interaction and charge recombination during the past decade, resulting in successful development of various dye structures with high efficiency.^{5e,f,h,8} On the other hand, the circle chain surrounding the dye molecule not only suppresses intermolecular interactions and charge recombination efficiently, but also immobilizes the conjugated backbone in a planar configuration, hence extending the absorption spectra for efficient light harvesting. However, only **LJ-3**, is an example of a dye bearing a circle chain embracing π -spacer that has been recently developed with a conversion efficiency of 8.34% recently.⁹ Many fundamental issues need to be investigated for further development of this promising kind of circle chain embracing D- π -A sensitizers for DSCs. The most urgent current issue that needs to be addressed is the energy level matching for efficient electron injection and dye regeneration,¹⁰ which is significant for the rational molecular design of this new type of organic dye.

In this context, we introduced various donor moieties (carbazole, indoline and dimethoxytriphenylamine) into the D- π -A system bearing a circle chain embracing π -spacer and cyanoacrylic acid as an acceptor, resulting in three new organic dyes **LJ-4**, **LJ-5** and **LJ-6** (Scheme 1), respectively. Essentially, these three new dyes were designed based on the following

^aPhotovoltaic Materials Unit, National Institute for Materials Science, Tsukuba, Ibaraki 305-0047, Japan. E-mail: HAN.Liyuan@nims.go.jp; Fax: +81 298592304; Tel: +81 298592747

^bState Key Laboratory of Metal Matrix Composites, Shanghai Jiao Tong University, 800 Dong Chuan RD. Minhang District, Shanghai 200240, China

† Electronic supplementary information (ESI) available: Spectra characterization, DFT calculations and HPLC analysis of dyes **LJ-4**, **LJ-5** and **LJ-6**. See DOI: 10.1039/c3ta12368e



Scheme 1 Molecular structures and synthetic routes of circle chain embracing D- π -A dyes **LJ-4**, **LJ-5** and **LJ-6**.

considerations: (1) further expanding the absorption spectra by introducing stronger electron donating parts for light harvesting; (2) tuning the energy levels of dye molecular orbitals and suggesting suitable driving forces for efficient electron injection and dye regeneration; (3) investigating the influence of the electron donating ability of various donor parts (indoline > dimethoxytriphenylamine > triphenylamine > carbazole) on the photovoltaic performance of DSCs based on circle chain embracing D- π -A dyes. The synthesis, spectra, electrochemical and photovoltaic properties of the dyes **LJ-4**, **LJ-5** and **LJ-6** have been investigated, and dye **LJ-3** (Scheme 1) is also presented for comparative analysis.

Results and discussion

Molecular design and synthesis

The preparation of three new circle chain embracing D- π -A dyes **LJ-4**, **LJ-5** and **LJ-6** was achieved *via* bromination, Suzuki coupling and Knoevenagel condensation reactions in a moderate yield by the rational synthetic routes depicted in Scheme 1. Bromination of the circle chain embracing bithiophene **1** by NBS produced the resulting compound **2**,¹¹ which was then coupled with 5-formylthiophene-2-boronic acid to yield aldehyde **3**,⁹ a common intermediate for the three new dyes. Suzuki coupling between aldehyde **3** and the corresponding borate reagents gave the dye precursors **4**, **5** and **6**, which were converted to dyes **LJ-4**, **LJ-5** and **LJ-6** as purple solids *via* the Knoevenagel condensation, respectively. The desired

dyes were characterized by ¹H and ¹³C NMR spectroscopy, as well as mass spectrometry. The purities of the circle chain embracing D- π -A dyes **LJ-4**, **LJ-5** and **LJ-6** were characterized by HPLC analysis (Fig. S6–S8, ESI[†]).

UV-visible absorption spectra

The absorption spectra of the circle chain embracing D- π -A dyes **LJ-3**, **LJ-4**, **LJ-5** and **LJ-6** in dichloromethane are shown in Fig. 1, and the data is summarized in Table 1. Being similar to dye **LJ-3**, the three new dyes **LJ-4**, **LJ-5** and **LJ-6** exhibit two

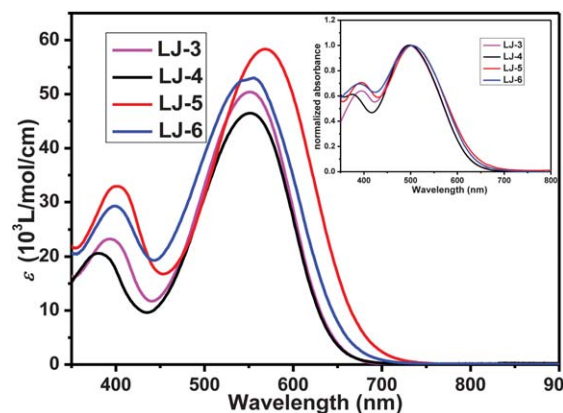


Fig. 1 Absorption spectra of dyes **LJ-3**, **LJ-4**, **LJ-5** and **LJ-6** in CH_2Cl_2 (2×10^{-5} M); normalized absorption spectra of **LJ-3**, **LJ-4**, **LJ-5** and **LJ-6** anchored on a $4 \mu\text{m}$ transparent TiO_2 film (inset).

Table 1 Optical and redox parameters of dyes **LJ-3**, **LJ-4**, **LJ-5** and **LJ-6**

Dye	^a $\lambda_{\text{max}}/\text{nm}$ ($\epsilon/\text{L mol}^{-1} \text{cm}^{-1}$)	^b $\lambda_{\text{max}}/\text{nm}$	^c S^{+0}/V (vs. NHE)	^d $S^{+*/\text{eV}}$ (vs. NHE)	^e E_{0-0}/V
LJ-3	551(50420), 393(23250)	496	0.81	1.10	1.91
LJ-4	550(46480), 380(20610)	496	0.94	-0.98	1.92
LJ-5	570(58300), 401(32940)	510	0.72	-1.21	1.93
LJ-6	556(53010), 399(29250)	506	0.76	-1.18	1.94

^a The absorption spectra were measured in CH_2Cl_2 solution (2×10^{-5} M). ^b Measured on TiO_2 film. ^c The S^{+0} corresponding to the ground-state oxidation potential (vs. NHE) in CH_2Cl_2 internally calibrated with ferrocene. ^d $S^{+*/\text{eV}} = S^{+0} - E_{0-0}$, where E_{0-0} is the zero-zero transition energy. ^e E_{0-0} values were estimated from the intersection between the normalized absorption and emission spectra in CH_2Cl_2 (Fig. S1, ESI †).

distinct absorption bands: one absorption band is in the UV region (360–430 nm) corresponding to the $\pi-\pi^*$ electron transitions of the conjugated molecules, as well as the overlapping $n-\pi^*$ electron transitions; and the other is in the visible region (500–600 nm) that can be assigned to intramolecular charge transfer (ICT) from the donating unit to the cyanoacrylic acid anchoring moiety. The maxima absorption peaks (λ_{max}) of the dyes vary: indoline dye **LJ-5** (570 nm) > dimethoxytriphenylamine dye **LJ-6** (556 nm) > triphenylamine dye **LJ-3** (551 nm) \approx carbazole dye **LJ-4** (550 nm), which could be explained by the strength of the electron donating ability of the donor group in each dye.¹² Due to the relatively stronger electron donating ability of the indoline moiety, the ICT transitions absorption band in indoline dye **LJ-5** is redshifted ~ 20 nm relative to those of the carbazole dye **LJ-4** and dimethoxytriphenylamine dye **LJ-6**, and with enhancement of molar extinction coefficient (ϵ). Circle chain embracing D- π -A dyes **LJ-4**, **LJ-5** and **LJ-6** exhibit similar emission in CH_2Cl_2 solution but different Stokes shifts (Fig. S1, ESI †). Among these three new dyes, the carbazole dye **LJ-4** exhibits the largest Stokes shift, which indicates significant structural reorganization of the dye molecule upon photoexcitation.¹³

The normalized UV-vis absorption spectra of these dyes adsorbed on TiO_2 films are shown in the inset in Fig. 1. The λ_{max} for the dye-loaded TiO_2 films are also listed in Table 1. After being adsorbed on the TiO_2 film, **LJ-3**, **LJ-4**, **LJ-5** and **LJ-6** show fine absorption peaks, similar to those in solution, suggesting that the steric hindrance of the insulating outer ring suppresses the intermolecular interactions effectively. The maximum absorption of these dyes anchored on the TiO_2 film exhibits a hypochromatic shift of approximately 50 nm in comparison with that in solution. Such a blue shift could be assigned to the solvent effect and/or deprotonation of the carboxylic acid in the anchoring process.¹⁴ As compared to the analogue dye MK-2 containing four thiophene units linked long alkyl chains,^{2c,15} carbazole dye **LJ-4** exhibits obvious red-shift both in solution and on TiO_2 film, as well as higher ϵ under the same conditions (Fig. S2 and S3, ESI †), even though dye **LJ-4** only possesses three thiophene units. The results further indicate that employing a circle chain to fix the conjugated backbone was an efficient way to improve the light harvesting efficiency.

Electrochemical properties and energy levels

The electrochemical properties of the circle chain embracing D- π -A dyes **LJ-3**, **LJ-4**, **LJ-5** and **LJ-6** were studied by cyclic

voltammetry (CV) in CH_2Cl_2 containing 0.1 M tetra-*n*-butylammonium hexafluorophosphate (TBAHFP) as a supporting electrolyte. As shown in Fig. 2a, all these dyes exhibit two reversible oxidative waves. The different electron-donor moieties in **LJ-3**, **LJ-4**, **LJ-5** and **LJ-6** influence their first oxidation potentials, respectively. The HOMO levels corresponding to the first oxidation potentials (vs. NHE) increase in the order of indoline dye **LJ-5** (0.72 V) < dimethoxytriphenylamine dye **LJ-6** (0.76 V) < triphenylamine **LJ-3** (0.81 V) < carbazole dye **LJ-4** (0.94 V), which was associated with the electron-donating ability of indoline > dimethoxytriphenylamine > triphenylamine > carbazole. They are all more positive than the Nernst potential of I^-/I_3^- redox couple (0.4 V vs. NHE), ensuring regeneration of the oxidized dyes by I^- after electron injection, with the driving force of 0.41 V, 0.54 V, 0.32 V and 0.36 V for **LJ-3**, **LJ-4**, **LJ-5** and **LJ-6**, respectively (Fig. 2b). The excited state redox potentials of these three dyes (-0.98 to -1.21 V vs. NHE) are sufficiently more negative than the conduction band of TiO_2 (-0.5 V vs. NHE), ensuring sufficient driving force (0.48–0.71 V) for electron injection from the excited dyes to the conduction band of TiO_2 .

DFT calculations

To gain further insight into the molecular structure and frontier molecular orbitals of these new dyes, the geometries of dyes **LJ-4**, **LJ-5** and **LJ-6** were optimized by density functional theory (DFT) calculations at the B3LYP/6-31G** level. Fig. S4 (ESI †) displays the relative energies and electron distributions of the HOMOs and LUMOs of these dyes. The HOMOs are mainly delocalized from the donor parts to the oligothiophene π -spacer, whereas the LUMOs show localized electron distributions through the cyanoacrylic acid and its adjacent π -spacer. Hence, both orbitals provide sufficient overlap between the donor and acceptor to guarantee a fast charge transfer transition. Therefore, excitation from the HOMO to the LUMO should lead to efficient photoinduced electron transfer from the donor group to the TiO_2 film *via* the terminal cyanoacrylic acid. The optimized ground-state geometries and corresponding dihedral angles between each plane are shown in Fig. S5. † The circle chain embracing π -spacers in these three new dyes perform similar planar configuration with a dihedral angle below 1° between the corresponding thiophene units, which will facilitate the ICT transition, as suggested by their excellent absorption in visible region described above. The geometry results indicate that π -conjugations in this type of circle chain

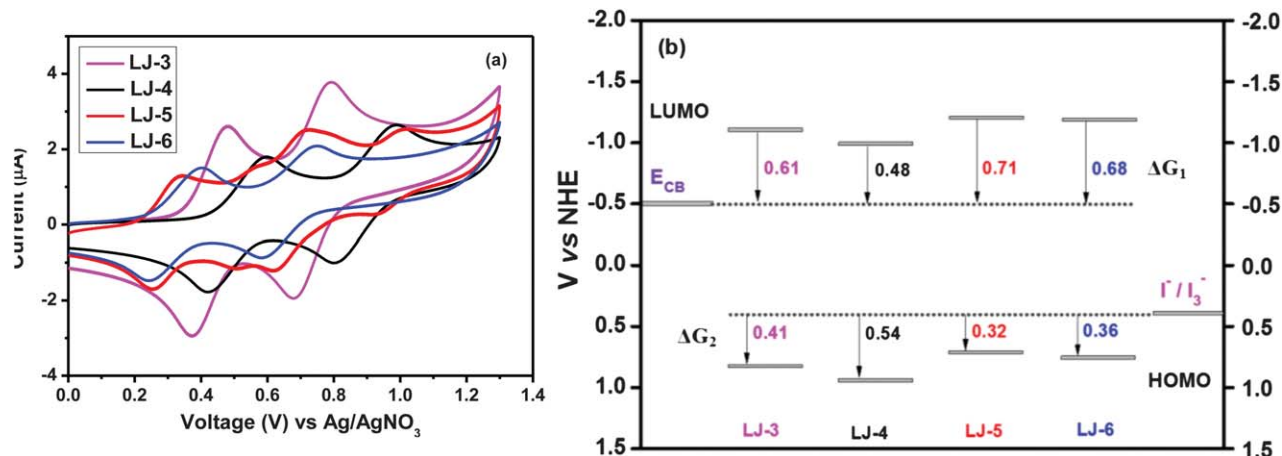


Fig. 2 (a) Cyclic voltammograms of dyes **LJ-3**, **LJ-4**, **LJ-5** and **LJ-6** in CH_2Cl_2 -TBAHFP (0.1 M), $[c] = 1 \times 10^{-4} \text{ mol L}^{-1}$, 293 K, scan rate = 100 mV s^{-1} ; (b) energy-level diagram of dyes **LJ-3**, **LJ-4**, **LJ-5** and **LJ-6**, the electrolyte and TiO_2 , E_{CB} : energy level of conduction band of TiO_2 ; ΔG_1 : driving force for electron injection; ΔG_2 : driving force for regeneration of the oxidized dyes.

embracing D- π -A dyes are not altered by their donor moieties, which is convenient for molecular tailoring.

Photovoltaic properties

The photovoltaic characteristics of the DSCs based on these dyes under AM1.5G condition (100 mW cm^{-2}) have been investigated,¹⁶ employing a solution of 0.6 M 1-propyl-2,3-dimethylimidazolium iodide, 0.05 M I_2 , 0.1 M LiI and 0.5 M *tert*-butylpyridine (TBP) in acetonitrile as the electrolyte. The onset wavelength of the IPCE spectra shift towards the red region was in the order **LJ-4** \approx **LJ-3** < **LJ-6** < **LJ-5** cells (Fig. 3), in accordance with the absorption spectra observed for the dye-loaded TiO_2 films. Comparing with the maximum IPCE value (83%) observed in the range of 400–600 nm for the DSCs based on triphenylamine dye **LJ-3**, the maximum value of IPCE for carbazole dye **LJ-4** increases to 88%, whereas those for indoline dye **LJ-5** and dimethoxytriphenylamine dye **LJ-6** decrease to 77% and 81%, respectively. Considering the IPCE results together with the energy levels of these four circle chain embracing D- π -A dyes, the IPCE values vary in the order of **LJ-5**-based cells (77%) < **LJ-6**-based cells (81%) < **LJ-3**-based cells (83%) < **LJ-4**-

based cells (88%), which is consistent with the driving force for the regeneration of the oxidized dye in the trend of indoline dye **LJ-5** (0.32 V) < dimethoxytriphenylamine dye **LJ-6** (0.36 V) < triphenylamine dye **LJ-3** (0.41 V) < carbazole dye **LJ-4** (0.54 V) (Fig. 2b). The results indicate that a negative shift of the ground-state oxidation potential might dominate the slower regeneration of the oxidized state of dyes **LJ-5** and **LJ-6** by the Γ^- in the redox electrolyte. Among these four circle chain embracing D- π -A dyes, carbazole dye **LJ-4** possesses the lowest driving force (0.48 V) for electron injection, but the DSCs based on dye **LJ-4** gave the highest IPCE, indicating that a driving force of 0.48 V is sufficient for electron injection from the excited dyes to the conduction band of TiO_2 . As a result, among these four dyes, the energy levels of carbazole dye **LJ-4** match best with the conduction band of TiO_2 and the redox potential of the redox species for efficient electron injection and dye regeneration.

We plotted current–voltage curves and calculated the photovoltaic properties of the **LJ-3**, **LJ-4**, **LJ-5** and **LJ-6** cells under the same conditions (Fig. 4 and Table 2, respectively). The short-circuit currents (J_{SC}) vary in the order of **LJ-3**-based cells (15.03 mA cm^{-2}) < **LJ-6**-based cells (15.67 mA cm^{-2})

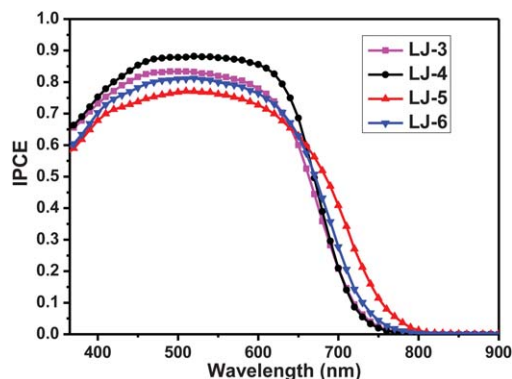


Fig. 3 IPCE spectra of DSCs based on dyes **LJ-3**, **LJ-4**, **LJ-5** and **LJ-6**.

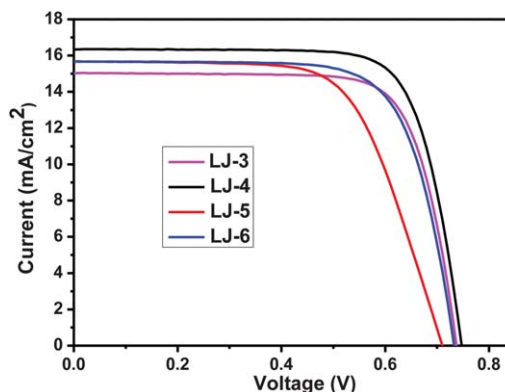


Fig. 4 J - V curves of DSCs based on **LJ-3**, **LJ-4**, **LJ-5** and **LJ-6**.

Table 2 Photovoltaic performance for DSCs based on dyes **LJ-3**, **LJ-4**, **LJ-5** and **LJ-6**^a

DSC	IPCE _{max} [%]	J_{SC} [mA cm ⁻²]	V_{OC} [V]	FF	η [%]	Dye-loading amount [10 ⁻⁷ mol cm ⁻²]
LJ-3	83	15.03	0.737	0.752	8.34	1.74
LJ-4	88	16.34	0.747	0.754	9.20	1.85
LJ-5	77	15.68	0.710	0.667	7.42	1.44
LJ-6	81	15.67	0.732	0.723	8.29	1.65

^a Measurements were performed under AM1.5 irradiation of the DSC devices with a 0.2304 cm² active surface. J_{SC} , short circuit current; V_{OC} , open circuit voltage; FF, fill factor; η , conversion efficiency.

≈ **LJ-5**-based cells (15.68 mA cm⁻²) < **LJ-4**-based cells (16.34 mA cm⁻²). The slightly larger J_{SC} of the DSCs based on **LJ-5** and **LJ-6**, in comparison with that of DSCs based on **LJ-3**, demonstrates the beneficial influence of the red-shifted absorption spectra of **LJ-5** and **LJ-6** on TiO₂ film and the broadening of the IPCE spectra of the **LJ-5** cells and **LJ-6** cells. The high J_{SC} observed for the **LJ-4** cells is attributed to its high IPCE value in the range of 400–600 nm. The open-circuit voltages (V_{OC}) of the DSCs based on circle chain embracing D- π -A dyes **LJ-4**, **LJ-5** and **LJ-6** were 0.747 V, 0.710 V and 0.732 V, respectively. The V_{OC} values of all these cells are comparable to those of alkylated dyes, such as MK-2 (~0.73 V).^{2c,15} This implies that the circle chain surrounding the dye backbone is effective in suppressing charge recombination between the injected electron in TiO₂ and I₃⁻ in electrolyte. As a result, DSCs based on the three new circle chain embracing D- π -A dyes **LJ-4**, **LJ-5** and **LJ-6** show overall conversion efficiencies of 9.20%, 7.42% and 8.29%, respectively.

CEM and IMVS characterization

The V_{OC} is related to the conduction band position of TiO₂ and the charge recombination rate in DSCs.¹⁷ In order to understand the difference of the V_{OC} observed for the DSCs based on the circle chain embracing D- π -A dyes **LJ-4**, **LJ-5** and **LJ-6**, the relative conduction band positions and electron lifetimes in the DSCs based on the corresponding sensitizers were investigated. Firstly, we measured the relative conduction band position of TiO₂ through a charge extraction method (CEM) reported by Frank *et al.*¹⁸ As shown in Fig. 5, the DSCs based on circle

chain embracing D- π -A dyes **LJ-4**, **LJ-5** and **LJ-6** exhibit an approximately linear increase in V_{OC} as a function of the logarithm of electron density. Under the same condition, the CEM plots for DSCs based on these three dyes almost overlap, indicating that DSCs based on **LJ-4**, **LJ-5** and **LJ-6** share the similar conduction band position. The results suggest that the adjustment of donor parts in this type of organic sensitizer has less influence on the shift of the conduction band of TiO₂. Therefore, the V_{OC} difference of DSCs based on **LJ-4**, **LJ-5** and **LJ-6** would be caused by their various charge recombination rates, which were confirmed by the measurement of electron lifetimes (τ_e) in the conduction band of TiO₂ by means of intensity-modulated photovoltage spectroscopy (IMVS). As shown in Fig. 6, at a fixed voltage, the τ_e values of the DSCs based on these three dyes vary in the order of **LJ-5** < **LJ-6** < **LJ-4**, suggesting that the higher dye-loading amount (Table 2) results in a denser dye layer formed on the TiO₂ surface, which may be effective in the suppression of charge recombination between I₃⁻ and the injected electron in TiO₂. The various dye loading amounts observed for the circle chain embracing D- π -A dyes **LJ-3**, **LJ-4**, **LJ-5** and **LJ-6** may be caused by their different solubility and/or sizes of donor moieties. The different solubility is associated with the different polarity of dye molecules resulting from the varying donating abilities of donor moieties.

EIS characterization

To obtain further insight into the important interfacial charge transfer processes in DSCs based on circle chain embracing

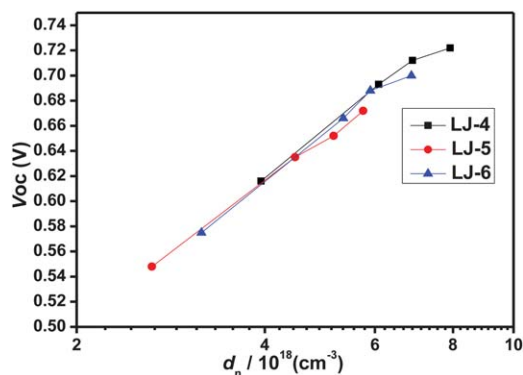


Fig. 5 Charge density at open circuit as a function of V_{OC} for the DSCs based on dyes **LJ-4**, **LJ-5** and **LJ-6**.

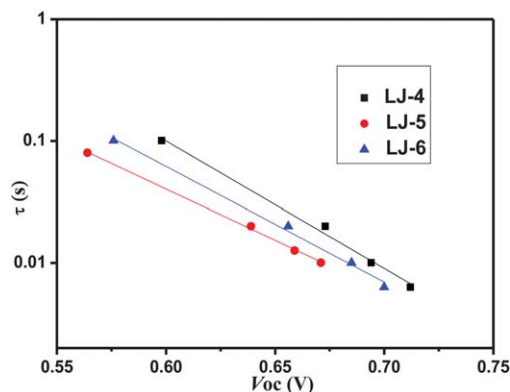


Fig. 6 Electron lifetime (τ_e) as a function of V_{OC} for the DSCs based on dyes **LJ-4**, **LJ-5** and **LJ-6**.

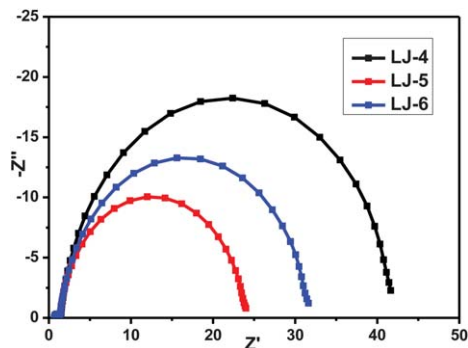


Fig. 7 EIS Nyquist plots for DSCs based on dyes **LJ-4**, **LJ-5** and **LJ-6** under dark (-0.65 V).

D- π -A dyes **LJ-4**, **LJ-5** and **LJ-6**, electrochemical impedance spectroscopy (EIS) was performed in the dark under a forward bias of -0.65 V with a frequency range of 10^{-1} Hz to 10^6 Hz. Generally, three semicircles are observed in EIS Nyquist plots (Fig. 7). The small and large semicircles located at the high- and middle-frequency regions, which are attributed to the redox reaction resistance at the platinum counter electrode, and the electron transfer resistance at the TiO_2 /dye/electrolyte interface (R_{rec}), respectively.¹⁹ Another small semicircle located at the low-frequency region corresponding to the Warburg diffusion process resistance of I^-/I_3^- in the electrolyte often overlap with the middle-frequency large semicircle, probably due to the low viscosity of the solvents used in our electrolytes, and the shorter length for I^- ion diffusion as only the thin spacer was used.²⁰ For the same counter electrode and electrolyte, a similar diameter semicircle was obtained at the low frequency region. At the middle frequency region, the semicircle diameter is responsible for the charge recombination, which is associated with the structure of the sensitizer and interfacial engineering. The R_{rec} values for the DSCs based on **LJ-4**, **LJ-5** and **LJ-6** are $40 \Omega \text{ cm}^2$, $23 \Omega \text{ cm}^2$ and $31 \Omega \text{ cm}^2$, respectively. Thus it can be concluded that the surface blocking effect of these circle chain embracing D- π -A dyes decreases in the order of **LJ-4** > **LJ-6** > **LJ-5**, as suggested by their dye-loading amount on TiO_2 film. The trend is in accordance with the decreasing sequence of the V_{OC} of the DSCs.

Conclusion

In summary, we successfully developed three new D- π -A dyes **LJ-4**, **LJ-5** and **LJ-6** bearing circle chain embracing oligothiophene as a π -spacer and cyanoacrylic acid as the acceptor moieties for high-efficiency DSCs. DSCs employing the sensitizer **LJ-4** and the iodine redox electrolyte exhibit a good power conversion efficiency of 9.20% measured under 100 mW cm^{-2} , simulated AM1.5 sunlight, while DSCs based on indoline dye **LJ-5** and dimethoxytriphenylamine dye **LJ-6** show a slightly lower efficiency of 7.42% and 8.29%, respectively, due to their less positive ground-state oxidation potentials resulting in slower regeneration of the oxidized state of **LJ-5** and **LJ-6** by the I^- in the redox electrolyte. The dissimilarity of the cells'

photovoltages is scrutinized by evaluating the titania conduction band and the variation of interfacial charge recombination kinetics. Among these three dyes, the energy levels of carbazole dye **LJ-4** match best with the conduction band of TiO_2 and the redox potential of the redox species for efficient electron injection and dye regeneration. The presented results further demonstrate that employing a circle chain embracing π -spacer is a promising strategy to construct efficient organic sensitizers for DSCs. Our work will attract the increasing attention of researchers in the same field, and provide enlightenment for further molecular design of this type of organic dye.

Experimental

Materials and instruments

All chemicals and reagents were used as received from chemical companies without further purification. Anhydrous solvents were degassed by Ar bubbling for 20 min before use. Compound **3** was synthesized according to our previous method.¹⁰ Column chromatography was performed with Wakogel-C300 as a stationary phase. UV-Vis spectra were measured in CH_2Cl_2 solution or TiO_2 film using a UV-3600 Spectrophotometer (SHIMADZU). Cyclic voltammetry (CV) was performed on a CH Instruments 624D potentiostat/galvanostat system. All CV measurements were carried out in anhydrous CH_2Cl_2 containing 0.1 M TBAHFP as a supporting electrolyte, purging with argon prior to conducting the experiment. A platinum electrode was used as a working electrode, Ag/AgNO_3 in saturated $\text{KNO}_3(\text{aq.})$ as a reference electrode, and a platinum wire as a counter electrode. The mass spectra were measured on a Shimadzu Biotech matrix-assisted laser desorption ionization (MALDI) mass spectrometer. The ^1H - and ^{13}C -NMR measurements were performed by a DRX-600 spectrometer (Bruker BioSpin). Incident photon-to-current conversion efficiency spectra were measured by a CEP-200BX spectrometer (Bunko Keiki). The current-voltage (I - V) curves were obtained by a WXS-90S-L2 Super solar simulator (WACOM).

Synthesis and characterization

Preparation of compound 4. To a stirred solution of compound **3** (80 mg, 0.109 mmol) in 1,4-dioxane (20 mL) was added 9-ethyl-9H-carbazol-3-ylboronic acid (70 mg, 0.218 mmol), potassium carbonate (60 mg, 0.436 mmol), H_2O (5 mL), followed by $\text{Pd}(\text{PPh}_3)_4$ (24 mg, 0.02 mmol). The resulting mixture was stirred at 90°C under argon atmosphere for 12 h. The solvent was evaporated under reduced pressure and the residue was treated with water (30 mL), extracted twice with CH_2Cl_2 (30 mL \times 2). The organic layers were combined and washed twice with water and once with brine, dried over anhydrous sodium sulfate. After removing the solvent under reduced pressure, the residue was loaded onto a silica gel column with PE-EA (5/1, v/v) as the eluent to afford the desired compound **4** as an orange solid (68 mg, 74%). ^1H NMR (CDCl_3 , 600 MHz), δ : 9.80 (s, 1H), 8.19 (s, 1H), 8.04 (d, $J = 7.8$ Hz, 1H), 7.59 (d, $J = 3.6$ Hz, 1H), 7.54 (d, $J = 9.0$ Hz, 1H), 7.46–7.51 (m, 3H), 7.40 (d, $J = 8.4$ Hz, 1H), 7.34 (d, $J = 8.4$ Hz, 1H), 7.24

(d, $J = 6.6$ Hz, 1H), 7.14 (s, 1H), 7.13 (s, 1H), 7.02 (d, $J = 2.4$ Hz, 1H), 6.76 (d, $J = 9.0$ Hz, 4H), 4.36 (q, $J = 7.2$ Hz, 2H), 4.11–4.15 (m, 4H), 3.76–3.84 (m, 4H), 1.52–1.59 (m, 8H), 1.42 (t, $J = 7.2$ Hz, 1H), 1.25–1.32 (m, 4H), 0.94–1.03 (m, 4H). ^{13}C NMR (CDCl_3 , 150 MHz), δ : 182.30, 158.94, 158.72, 148.68, 143.04, 140.40, 14.35, 139.30, 137.63, 136.32, 134.01, 132.47, 132.13, 131.69, 130.90, 130.81, 130.72, 129.12, 125.95, 125.72, 124.71, 123.59, 123.25, 122.90, 122.77, 120.48, 119.04, 117.04, 116.65, 116.08, 108.64, 108.59, 107.06, 106.90, 69.85, 38.74, 30.35, 27.54. ESI (m/z): calcd for $\text{C}_{51}\text{H}_{47}\text{NO}_5\text{S}_3$, 849.26 (M^+); found, 849.26.

Preparation of compound 5. To a stirred solution of compound 3 (80 mg, 0.109 mmol) in 1,4-dioxane (20 mL) was added 4-phenyl-1,2,3,3a,4,8b-hexahydrocyclopenta[*b*]indol-7-ylboronic acid (80 mg, 0.218 mmol), potassium carbonate (60 mg, 0.436 mmol), H_2O (5 mL), followed by $\text{Pd}(\text{PPh}_3)_4$ (24 mg, 0.02 mmol). The resulting mixture was stirred at 90 °C under argon atmosphere for 12 h. Evaporation of the solvent under reduced pressure and the residue was treated with water (30 mL), extracted twice with CH_2Cl_2 (30 mL \times 2). The organic layers were combined and washed twice with water and once with brine and dried over anhydrous sodium sulfate. After removing the solvent under reduced pressure, the residue was loaded onto a silica gel column with PE-EA (5/1, v/v) as eluent to afford the desired compound 5 as an orange solid (69 mg, 71%). ^1H NMR (CDCl_3 , 600 MHz), δ : 9.79 (s, 1H), 7.62 (s, 1H), 7.45 (t, $J = 4.2$ Hz, 1H), 7.43 (t, $J = 4.2$ Hz, 1H), 7.31–7.36 (m, 2H), 7.03–7.11 (m, 2H), 6.90–7.01 (m, 5H), 6.70–6.73 (m, 5H), 4.71–4.80 (m, 1H), 4.08–4.11 (m, 4H), 3.75–3.80 (m, 5H), 2.01–2.06 (m, 1H), 1.92–1.96 (m, 1H), 1.81–1.87 (m, 2H), 1.51–1.67 (m, 8H), 1.22–1.28 (m, 4H), 0.96–0.99 (m, 4H). ^{13}C NMR (CDCl_3 , 150 MHz), δ : 182.23, 158.91, 158.69, 148.72, 146.62, 142.92, 142.59, 140.30, 137.58, 136.39, 135.64, 133.92, 131.93, 131.52, 130.73, 130.63, 130.05, 129.19, 129.12, 125.48, 124.58, 123.90, 122.69, 121.68, 121.51, 119.17, 116.67, 116.10, 108.18, 107.01, 106.89, 106.83, 69.83, 45.36, 34.69, 33.90, 31.59, 30.36, 27.52, 24.45, 22.66, 14.12. ESI (m/z): calcd for $\text{C}_{54}\text{H}_{51}\text{NO}_5\text{S}_3$, 889.29 (M^+); found, 889.29.

Preparation of compound 6. To a stirred solution of compound 3 (80 mg, 0.109 mmol) in 1,4-dioxane (20 mL) was added 4-dimethoxyphenylaminophenylboronic acid (94 mg, 0.218 mmol), potassium carbonate (60 mg, 0.436 mmol), H_2O (5 mL), followed by $\text{Pd}(\text{PPh}_3)_4$ (24 mg, 0.02 mmol). The resulting mixture was stirred at 90 °C under argon atmosphere for 12 h. The solvent was evaporated under reduced pressure and the residue was treated with water (30 mL) and extracted twice with CH_2Cl_2 (30 mL \times 2). The organic layers were combined and washed twice with water and once with brine and dried over anhydrous sodium sulfate. After removing the solvent under reduced pressure, the residue was loaded onto a silica gel column with PE-EA (5/1, v/v) as the eluent to afford the desired compound 6 as an orange solid (77 mg, 74%). ^1H NMR (CDCl_3 , 600 MHz), δ : 9.77 (s, 1H), 7.56 (d, $J = 4.2$ Hz, 1H), 7.44 (t, $J = 8.4$ Hz, 1H), 7.39 (t, $J = 8.4$ Hz, 1H), 7.21 (d, $J = 9.0$ Hz, 2H), 7.09 (s, 1H), 7.03 (d, $J = 9.0$ Hz, 4H), 6.98 (d, $J = 4.2$ Hz, 1H), 6.94 (s, 1H), 6.83 (d, $J = 8.4$ Hz, 2H), 6.80 (d, $J = 9.0$ Hz, 4H), 6.70 (d, $J = 8.4$ Hz, 2H), 6.67 (d, $J = 8.4$ Hz, 2H), 4.07–4.13 (m, 4H), 3.78 (s, 6H), 3.73–3.76 (m, 4H), 1.48–1.54 (m, 8H), 1.23–1.26 (m, 4H), 0.98–

0.99 (m, 4H). ^{13}C NMR (CDCl_3 , 150 MHz), δ : 182.27, 158.85, 158.68, 155.99, 148.63, 147.93, 141.75, 140.70, 140.36, 137.62, 136.21, 134.01, 132.20, 131.75, 130.82, 130.75, 130.68, 129.10, 126.61, 125.75, 124.60, 122.78, 120.50, 116.47, 116.01, 114.75, 106.93, 106.82, 69.79, 55.52, 31.78, 27.61, 27.53. ESI (m/z): calcd for $\text{C}_{57}\text{H}_{53}\text{NO}_7\text{S}_3$, 959.30 (M^+); found, 959.30.

Preparation of dye LJ-4. A solution of aldehyde 4 (60 mg, 0.071 mmol), cyanoacetic acid (18 mg, 0.212 mmol), piperidine (36 mg, 0.424) in CHCl_3 (15 mL) was stirred at reflux for 10 h. The reaction mixture was cooled to room temperature, then treated with water (30 mL) and acidified with 1 M aqueous hydrochloric acid (10 mL) and extracted twice with CHCl_3 (30 mL \times 2). The organic layers were combined and washed twice with water and once with brine and dried over anhydrous sodium sulfate. After removing the solvent under reduced pressure, the residue was loaded onto a silica gel column with CH_2Cl_2 – CH_3OH (15/1, v/v) as eluent to afford the desired dye LJ-4 as a purple solid (56 mg, 87%). ^1H NMR (DMSO-d_6 , 600 MHz), δ : 8.34 (d, $J = 1.8$ Hz, 1H), 8.31 (s, 1H), 8.12 (d, $J = 7.8$ Hz, 1H), 7.84 (s, 1H), 7.61 (d, $J = 9.0$ Hz, 2H), 7.57 (t, $J = 8.4$ Hz, 1H), 7.46–7.50 (m, 2H), 7.40 (dd, $J_1 = 1.8$ Hz, $J_2 = 8.4$ Hz, 1H), 7.21–7.25 (m, 4H), 6.89 (d, $J = 8.4$ Hz, 2H), 6.86 (d, $J = 8.4$ Hz, 2H), 4.44 (q, $J = 7.2$ Hz, 2H), 4.10–4.12 (m, 4H), 3.74–3.81 (m, 4H), 1.41–1.46 (m, 8H), 1.30 (t, $J = 7.2$ Hz, 3H), 1.14–1.19 (m, 4H), 0.94–0.97 (m, 4H). ^{13}C NMR (DMSO-d_6 , 150 MHz), δ : 158.84, 142.54, 140.55, 139.46, 134.61, 132.86, 131.55, 131.48, 130.35, 129.68, 126.67, 125.40, 125.16, 124.00, 123.23, 123.16, 122.52, 120.94, 119.55, 116.89, 116.32, 115.76, 110.21, 109.87, 107.67, 107.47, 69.60, 37.55, 30.33, 27.54, 27.49, 14.12. ESI (m/z): calcd for $\text{C}_{54}\text{H}_{48}\text{N}_2\text{O}_6\text{S}_3$, 916.27 (M^+); found, 916.26.

Preparation of dye LJ-5. A solution of aldehyde 5 (60 mg, 0.067 mmol), cyanoacetic acid (17 mg, 0.2 mmol), piperidine (34 mg, 0.4) in CHCl_3 (15 mL) was stirred at reflux for 10 h. The reaction mixture was cooled to room temperature, then treated with water (30 mL) and acidified with 1 M aqueous hydrochloric acid (10 mL) and extracted twice with CHCl_3 (30 mL \times 2). The organic layers were combined and washed twice with water and once with brine, and dried over anhydrous sodium sulfate. After removing the solvent under reduced pressure, the residue was loaded onto a silica gel column with CH_2Cl_2 – CH_3OH (15/1, v/v) as eluent to afford the desired dye LJ-5 as a purple solid (52 mg, 81%). ^1H NMR (DMSO-d_6 , 600 MHz), δ : 8.35 (s, 1H), 7.86 (s, 1H), 7.50 (t, $J = 8.4$ Hz, 1H), 7.24–7.36 (m, 7H), 7.03 (s, 1H), 6.96–6.99 (m, 2H), 6.92 (d, $J = 8.4$ Hz, 1H), 6.83–6.85 (m, 4H), 4.83 (t, $J = 7.8$ Hz, 1H), 4.08–4.10 (m, 4H), 3.81 (t, $J = 8.4$ Hz, 1H), 3.73–3.76 (m, 4H), 2.00–2.02 (m, 1H), 1.84–1.87 (m, 1H), 1.78–1.82 (m, 1H), 1.72–1.74 (m, 1H), 1.61–1.64 (m, 1H), 1.41–1.48 (m, 8H), 1.31–1.38 (m, 1H), 1.15–1.18 (m, 4H), 0.85–0.88 (m, 4H). ^{13}C NMR (DMSO-d_6 , 150 MHz), δ : 158.76, 146.61, 142.67, 142.26, 136.34, 134.63, 132.68, 131.44, 131.25, 129.76, 129.55, 124.88, 124.59, 123.97, 121.76, 121.69, 119.08, 116.28, 115.77, 108.41, 107.61, 107.50, 107.43, 69.56, 68.60, 45.04, 34.85, 33.82, 30.31, 27.51, 24.43. ESI (m/z): calcd for $\text{C}_{57}\text{H}_{52}\text{N}_2\text{O}_6\text{S}_3$, 956.30 (M^+); found, 956.29.

Preparation of LJ-6. A solution of aldehyde 6 (60 mg, 0.063 mmol), cyanoacetic acid (17 mg, 0.2 mmol), and piperidine (34 mg, 0.4) in CHCl_3 (15 mL) was stirred at reflux for 10 h. The

reaction mixture was cooled to room temperature, then treated with water (30 mL), acidified with 1 M aqueous hydrochloric acid (10 mL) and extracted twice with CHCl_3 (30 mL \times 2). The organic layers were combined and washed twice with water and once with brine, dried over anhydrous sodium sulfate. After removing the solvent under reduced pressure, the residue was loaded onto a silica gel column with CH_2Cl_2 - CH_3OH (15/1, v/v) as eluent to afford the desired dye LJ-6 as a purple solid (54 mg, 85%). ^1H NMR (DMSO- d_6 , 600 MHz), δ : 8.22 (s, 1H), 7.64 (s, 1H), 7.44 (t, $J = 8.4$ Hz, 1H), 7.37 (t, $J = 8.4$ Hz, 1H), 7.22 (d, $J = 8.4$ Hz, 2H), 7.13 (s, 1H), 7.03 (d, $J = 9.0$ Hz, 4H), 6.95–6.96 (m, 2H), 6.81–6.85 (m, 6H), 6.71 (d, $J = 8.4$ Hz, 2H), 6.65 (d, $J = 8.4$ Hz, 2H), 4.09–4.12 (m, 4H), 3.79 (s, 6H), 3.71–3.76 (m, 4H), 1.41–1.49 (m, 8H), 1.16–1.20 (m, 4H), 0.94–0.99 (m, 4H). ^{13}C NMR (DMSO- d_6 , 150 MHz), δ : not sufficiently soluble to obtain a spectrum. ESI (m/z): calcd for $\text{C}_{60}\text{H}_{54}\text{N}_2\text{O}_8\text{S}_3$, 1026.30 (M^+); found, 1026.29.

Cell fabrication and characterization

The photoanode (thickness 19 μm ; area 0.25 cm^2) of the DSC was a double-layered TiO_2 film containing a transparent layer 14 μm thick with titania particles (~ 20 nm) and a scattering layer 6 μm thick (400 nm nanoparticles). The double-layered film was heated to 520 $^\circ\text{C}$, sintered for 1 hour and then cooled to *ca.* 80 $^\circ\text{C}$ and treated with 0.1 M HCl aqueous. After the HCl treatment, the films were washed, dried and then immersed in 3×10^{-4} M acetonitrile-*tert*-butyl alcohol (1/1, v/v) solution of the sensitizers for 40 h. Afterwards, the dye-loaded TiO_2 film and a platinum coated conducting glass were assembled into a sandwich type of DSC and sealed by heating the Surlyn spacer (40 mm thick). An electrolyte was injected into the spacer from the counter electrode side through a pre-drilled hole, and then the hole was sealed with a Bynel sheet and a thin-glass-slide cover by heating. The electrolyte was from a commercial source and composed of 0.6 M dimethylpropylimidazolium iodide, 0.05 M I_2 , 0.1 M LiI and 0.5 M TBP in acetonitrile. The adsorption amount of dyes on the surface of TiO_2 films, that were prepared under the same conditions as those fabricated into cells, was estimated as follows: TiO_2 films sensitized with dyes were immersed into 0.05 M NaOH in THF- H_2O (1/1, v/v) for desorption of the dyes. The amount of desorbed dye was evaluated by their corresponding absorbance spectra. Four pieces of TiO_2 film for one cell were tested and an average value was adopted.

The I - V characteristics were determined by using a black metal mask with an aperture area of 0.2304 cm^2 under standard AM 1.5 sunlight, 100 mW cm^{-2} (WXS-155S-10: Wacom Denso Co. Japan). Monochromatic IPCE spectra were measured with a monochromatic incident light of 1×10^{16} photons per cm^2 under 100 mW cm^{-2} in director current mode (CEP-2000BX, Bunko-Keiki). The IMVS were measured with a potentiostat (Solartron1287) equipped with a frequency response analyzer (Solartron1255B) at an open-circuit condition based on a monochromatic illumination (420 nm) controlled by a Lab-view system to obtain the photovoltaic response induced by the modulated light. The modulated light was driven with a 10% AC perturbation current superimposed on a DC current in a

frequency ranging from 10^{-1} to 10^6 Hz. The CEM was performed with the same monochromatic light source. The solar cell was illuminated at an open-circuit condition for 5 s to attain a steady state and then the light source was switched off when the device simultaneously switched to a short-circuit condition to extract the charges generated at that light intensity. The EIS spectra were measured with an impedance analyzer (Solartron Analytical, 1255B) connected with a potentiostat (Solartron Analytical, 1287) under illumination using a solar simulator (WXS-155S-10: Wacom Denso Co. Japan).

Acknowledgements

This work was supported by the Core Research for Evolutional Science and Technology (CREST) of the Japan Science and Technology Agency.

Notes and references

- 1 B. O'Regan and M. Grätzel, *Nature*, 1991, **353**, 737.
- 2 (a) M. K. Nazeeruddin, S. M. Zakeeruddin, R. Humphry-Baker, M. Jirousek, P. Liska, N. Vlachopoulos, V. Shklover, C.-H. Fischer and M. Grätzel, *Inorg. Chem.*, 1999, **38**, 6298; (b) M. K. Nazeeruddin, P. Péchy, T. Renouard, S. M. Zakeeruddin, R. Humphry-Baker, P. Comte, P. Liska, L. Cevey, E. Costa, V. Shklover, L. Spiccia, G. B. Deacon, C. A. Bignozzi and M. Grätzel, *J. Am. Chem. Soc.*, 2001, **123**, 1613; (c) N. Koumura, Z. S. Wang, S. Mori, M. Miyashita, E. Suzuki and K. Hara, *J. Am. Chem. Soc.*, 2006, **128**, 14256; (d) T. Bessho, S. M. Zakeeruddin, C.-Y. Yeh, E. W.-G. Diau and M. Grätzel, *Angew. Chem., Int. Ed.*, 2010, **49**, 6646; (e) H. N. Tsao, C. Yi, T. Moehl, J.-H. Yum, S. M. Zakeeruddin, M. K. Nazeeruddin and M. Grätzel, *ChemSusChem*, 2011, **4**, 591; (f) S. Cai, X. Hu, Z. Zhang, J. Su, X. Li, A. Islam, L. Han and H. Tian, *J. Mater. Chem. A*, 2013, **1**, 4763; (g) S. Zhang, X. Yang, Y. Numata and L. Han, *Energy Environ. Sci.*, 2013, **6**, 1443.
- 3 (a) N. Koide, A. Islam, Y. Chiba and L. Han, *J. Photochem. Photobiol., A*, 2003, **158**, 131; (b) Y. Tachibana, K. Hara, K. Sayama and H. Arakawa, *Chem. Mater.*, 2010, **22**, 1915; (c) J. N. Clifford, E. Palomares, M. K. Nazeeruddin, M. Grätzel, J. Nelson, X. Li, N. J. Long and J. R. Durrant, *J. Am. Chem. Soc.*, 2004, **126**, 5225; (d) A. Listorti, B. O'Regan and J. R. Durrant, *Chem. Mater.*, 2011, **23**, 3381; (e) S. Tatay, S. A. Haque, B. O'Regan, J. R. Durrant, W. J. H. Verhees, J. M. Kroon, A. Vidal-Ferran, P. Gavina and E. Palomares, *J. Mater. Chem.*, 2007, **17**, 3037; (f) S. Y. Huang, G. Schlichtho1rl, A. J. Nozik, M. Grätzel and A. J. Frank, *J. Phys. Chem. B*, 1997, **101**, 2576.
- 4 (a) Y. Chiba, A. Islam, Y. Watanabe, R. Komiyama, N. Koide and L. Y. Han, *Jpn. J. Appl. Phys.*, 2006, **45**, L638; (b) L. Y. Han, A. Islam, H. Chen, C. Malapaka, B. Chiranjeevi, S. Zhang, X. Yang and M. Yanagida, *Energy Environ. Sci.*, 2012, **5**, 6057.
- 5 (a) S. Kim, J. K. Lee, S. O. Kang, J. Ko, J. H. Yum, S. Fantacci, F. De Angelis, D. DiCenso, M. K. Nazeeruddin and M. Grätzel, *J. Am. Chem. Soc.*, 2006, **128**, 16701; (b) S. Ito, H. Miura, S. Uchida, M. Takata, K. Sumioka, P. Liska,

- P. Comte, P. Péchy and M. Grätzel, *Chem. Commun.*, 2008, 5194; (c) D. P. Hagberg, J.-H. Yum, H. Lee, F. De Angelis, T. Marinado, K. M. Karlsson, R. Humphry-Baker, L. Sun, A. Hagfeldt, M. Grätzel and M. K. Nazeeruddin, *J. Am. Chem. Soc.*, 2008, **130**, 6259; (d) G. Zhang, H. Bala, Y. Cheng, D. Shi, X. Lv, Q. Yu and P. Wang, *Chem. Commun.*, 2009, 2198; (e) Y. Bai, J. Zhang, D. Zhou, Y. Wang, M. Zhang and P. Wang, *J. Am. Chem. Soc.*, 2011, **133**, 11442; (f) W. Zeng, Y. Cao, Y. Bai, Y. Wang, Y. Shi, M. Zhang, F. Wang, C. Pan and P. Wang, *Chem. Mater.*, 2010, **22**, 1915; (g) W. Zhu, Y. Wu, S. Wang, W. Li, X. Li, J. Chen, Z.-S. Wang and H. Tian, *Adv. Funct. Mater.*, 2011, **21**, 756; (h) Y. Wu, M. Marszalek, S. M. Zakeeruddin, Q. Zhang, H. Tian, M. Grätzel and W. Zhu, *Energy Environ. Sci.*, 2012, **5**, 8261.
- 6 (a) Y.-S. Yen, H.-H. Chou, Y.-C. Chen, C.-Y. Hsu and J. T. Lin, *J. Mater. Chem.*, 2012, **22**, 8734; (b) B.-G. Kim, K. Chung and J. Kim, *Chem.-Eur. J.*, 2013, **19**, 5220.
- 7 (a) K. Hara, Z.-S. Wang, T. Sato, A. Furube, R. Katoh, H. Sugihara, Y. Dan-oh, C. Kasada, A. Shinpo and S. Suga, *J. Phys. Chem. B*, 2005, **109**, 15476; (b) Y. Numata, A. Islam, H. Chen and L. Han, *Energy Environ. Sci.*, 2012, **5**, 8548.
- 8 (a) S. Qu, C. Qin, A. Islam, Y. Wu, W. Zhu, J. Hua, H. Tian and L. Han, *Chem. Commun.*, 2012, **48**, 6972; (b) N. J. Ning, Y. Fu and H. Tian, *Energy Environ. Sci.*, 2010, **3**, 1170; (c) K. Pei, Y. Wu, A. Islam, Q. Zhang, L. Han, H. Tian and W. Zhu, *ACS Appl. Mater. Interfaces*, 2013, **5**, 4986; (d) C. Qin, A. Islam and L. Han, *J. Mater. Chem.*, 2012, **22**, 19236; (e) Y. Wu, X. Zhang, W. Li, Z.-S. Wang, H. Tian and W. Zhu, *Adv. Energy Mater.*, 2012, **2**, 149.
- 9 J. Liu, Y. Numata, C. Qin, A. Islam, X. Yang and L. Han, *Chem. Commun.*, 2013, DOI: 10.1039/c3cc41861h.
- 10 (a) G. Oskam, B. V. Bergeron, G. J. Meyer and P. C. Searson, *J. Phys. Chem. B*, 2001, **105**, 6867; (b) A. Islam, H. Sugihara and H. Arakawa, *J. Photochem. Photobiol., A*, 2003, **158**, 131.
- 11 K. Sugiyasu, Y. Honscho, R. M. Harrison, A. Sato, T. Yasuda, S. Seki and M. Takeuchi, *J. Am. Chem. Soc.*, 2010, **132**, 14754.
- 12 (a) B. Liu, W. Zhu, Q. Zhang, W. Wu, M. Xu, Z. Ning, Y. Xie and H. Tian, *Chem. Commun.*, 2009, 1766; (b) S. Kajiyama, Y. Uemura, H. Miura, K. Hara and N. Koumura, *Dyes Pigm.*, 2012, **92**, 1250; (c) M. Akhtaruzzaman, A. Islam, F. Yang, N. Asao, E. Kwon, S. P. Singh, L. Han and Y. Yamamoto, *Chem. Commun.*, 2011, **47**, 12400.
- 13 S. Haid, M. Marszalek, A. Mishra, M. Wielopolski, J. Teuscher, J.-E. Moser, R. Humphry-Baker, S. M. Zakeeruddin, M. Grätzel and P. Bäuerle, *Adv. Funct. Mater.*, 2012, **22**, 1291.
- 14 Y. Cui, Y. Wu, X. Lu, X. Zhang, G. Zhou, F. B. Miapheh, W. Zhu and Z.-S. Wang, *Chem. Mater.*, 2011, **23**, 4394.
- 15 Z.-S. Wang, N. Koumura, Y. Cui, M. Takahashi, H. Sekiguchi, A. Mori, T. Kubo, A. Furube and K. Hara, *Chem. Mater.*, 2008, **20**, 3993.
- 16 X. Yang, M. Yanagida and L. Han, *Energy Environ. Sci.*, 2013, **6**, 54.
- 17 (a) T. Marinado, K. Nonomura, J. Nissfolk, M. K. Karlsson, D. P. Hagberg, L. Sun, S. Mori and A. Hagfeldt, *Langmuir*, 2009, **26**, 2592; (b) J. Bisquert, D. Cahen, G. Hodes, S. Rühle and A. Zaban, *J. Phys. Chem. B*, 2004, **108**, 8106.
- 18 G. Schlichthoerl, S. Y. Huang, J. Sprague and A. J. Frank, *J. Phys. Chem. B*, 1997, **101**, 8141.
- 19 L. Han, N. Koide, Y. Chiba and T. Mitate, *Appl. Phys. Lett.*, 2004, **84**, 2433.
- 20 S.-R. Li, C.-P. Lee, H.-T. Kuo, K.-C. Ho and S.-S. Sun, *Chem.-Eur. J.*, 2012, **18**, 12085.